1-1-2018

3D Printed Electrodes for Improved Gas Reactant Transport for Electrochemical Reactions

Tania Benedetti Goncales
University of Wollongong, taniaben@uow.edu.au

Andrew Nattestad
University of Wollongong, anattest@uow.edu.au

Adam Taylor
University of Wollongong, taylora@uow.edu.au

Stephen T. Beirne
University of Wollongong, sbeirne@uow.edu.au

Gordon G. Wallace
University of Wollongong, gwallace@uow.edu.au

3D Printed Electrodes for Improved Gas Reactant Transport for Electrochemical Reactions

Abstract

Additive manufacturing (AM) techniques open up a range of new possibilities for the design of electrochemical systems, affording us the ability to overcome limitations and difficulties that traditional production processes face. Here we present a novel electrode design, realized through selective laser melting of metal powders, with an integrated gas (reactant) delivery system. This architecture results in significantly (~40%) enhanced hydrogen oxidation performance as compared with a control system. As such, this work serves as a proof-of-concept to highlight the wide array of designs that can be readily achieved due to recent developments in AM technologies.

Disciplines

Engineering | Physical Sciences and Mathematics

Publication Details

Benedetti, T., Nattestad, A., Taylor, A. C., Beirne, S. & Wallace, G. G. (2018). 3D Printed Electrodes for Improved Gas Reactant Transport for Electrochemical Reactions. 3D Printing and Additive Manufacturing, 5 (3), 215-219.

3D printed electrodes for improved gas reactant transport for electrochemical reactions

Tânia Machado Benedetti[1,2], Andrew Nattestad[1], Adam C. Taylor[1], Stephen Beirne[1], Gordon G. Wallace[1]*

1 – ARC Centre of Excellence for Electromaterials Science, Intelligent Polymer Research Institute, Australian Institute of Innovative Materials, Innovation Campus, University of Wollongong, Wollongong, NSW, 2522, Australia

2 – School of Chemistry, University of New South Wales, Sydney, Australia, 2052

* Corresponding author: gwallace@uow.edu.au

Abstract

Additive manufacturing techniques open up a range of new possibilities for the design of electrochemical systems, affording us the ability to overcome limitations and difficulties that traditional production processes face. Here we present a novel electrode design, realised through selective laser melting (SLM) of metal powders, with an integrated gas (reactant) delivery system. This architecture results in significantly (~40%) enhanced hydrogen oxidation performance, as compared to a control system. As such, this work serves as a proof-of-concept, to highlight the wide array of designs which can be readily achieved due to recent developments in additive manufacturing technologies.

Introduction

Additive manufacturing (AM), or three-dimensional printing (3D printing) allows rapid production of complex structures from software made models, using a wide array of materials, ranging from polymers [1-3] to metals [4-7] and even human cells [8-11]. As an alternative to traditional subtractive processes this offers the ability to produce structures with a complexity not attainable using conventional technologies, in particular the ability to create complex internal structures within 3D systems and creates new opportunities [12, 13]. Within the branch of AM, there has been an increasing focus towards energy based applications from the many techniques under this manufacturing style. Primarily, the creation of metal electrodes for sensing [14-17], and to a lesser extent, developments into conductive thermoplastic sensory structures.[18]

AM has already begun to bring specific benefit to electrochemistry, with the ability to build very large surface area structures an attractive aspect [19]. A number of different 3D printed electrodes and cell designs have been reported to date, such as interdigitated [20] and high surface area [21, 22] electrodes for energy applications, as well as synthetic reactors for microfluidics [23]. These recent contributions highlight that the use of such technology for electrochemical applications is still at a nascent stage, with opportunities to use these advances to increase the capabilities of electrochemical reactions and devices as AM decreases the gap between theoretical and experimental[24]. Moreover, it is considered that the advantages brought about through 3D printing has the potential to revolutionise energy materials and their applications in an efficiency impossible through traditional manufacturing [25].

Gas oxidation / reduction reactions are a major field of research [26, 27] with wide reaching practical benefit. There is however a trade-off between the advantages of high

surface area electrodes, *i.e.*, an increased number of active sites, and the challenge of getting the reactants to these sites. In such reactions, gas must be delivered into the electrolyte and then to the surface of the electrode in order to be oxidized/reduced. For practical applications, elegant alternatives for transport of the gas reactants are desired. The ability to control the delivery of reactants or removal of products through judicious 3D electrode design and fabrication offers an enormous promise as this can help overcome limitations which may arise from slow diffusion of reactants into a high surface area electrode. It should be noted that, at the research scale, such as in reaction mechanism studies, diffusion limitations may be overcome by using either rotating disk electrodes (RDE) or gas diffusion layers (GDL) loaded with catalyst. Obviously, RDE is not used in practical, large scale, devices and GDL are limited to 2D configurations, again not ideal for large scale reactions.

The hydrogen oxidation reaction (HOR), which takes place at the anode of fuel cells, involves fast electron transfer at the interface of platinum electrodes, under acidic conditions. The speed of this means that the reaction is typically severely limited by diffusion of the H_2 molecules to the electrode surface [28]. In the present work, we introduce a bespoke 3D printed metal electrode fabrication via SLM for electrochemical reactions involving gaseous reactants. This fabrication method has been selected due to its reliability in production of high resolution prints, as well as production of parts with a very high relative density and low porosity[29], making it ideal for fabrication of solid, complex electrode structures.

The electrode presented here was designed to improve gas delivery to the active catalytic sites of a porous scaffold structure and manufactured using selective laser melting of a titanium alloy (Ti6Al4V). This was then coated with a Pt catalyst by electrodeposition and the effect of designed gas delivery system on their HOR response was observed by linear sweep voltammetry (LSV). Other reactions involving gas molecules as reactants, like CO_2 reduction and oxygen reduction/oxidation reactions could also benefit from this new concept.

Results and Discussion

The electrode design (seen in Figure 1) consists of a cylindrical section comprising a body centre cubic based 3D scaffolded structure (beam element diameter 200 μm, lattice spacing 1000 μm), with a total height of 61.1 mm and diameter of 15.5 mm, with the addition to two connections at the top. One of these is for electrical contact and the other to connect a gas supply. Gas is distributed inside the electrode via a four-way gas splitter, with each internal tube having a diameter of 1.5 mm, with the ends of each terminating 2.54 mm above the bottom of the electrode. Detailed design and melting parameters can be found in the experimental section.

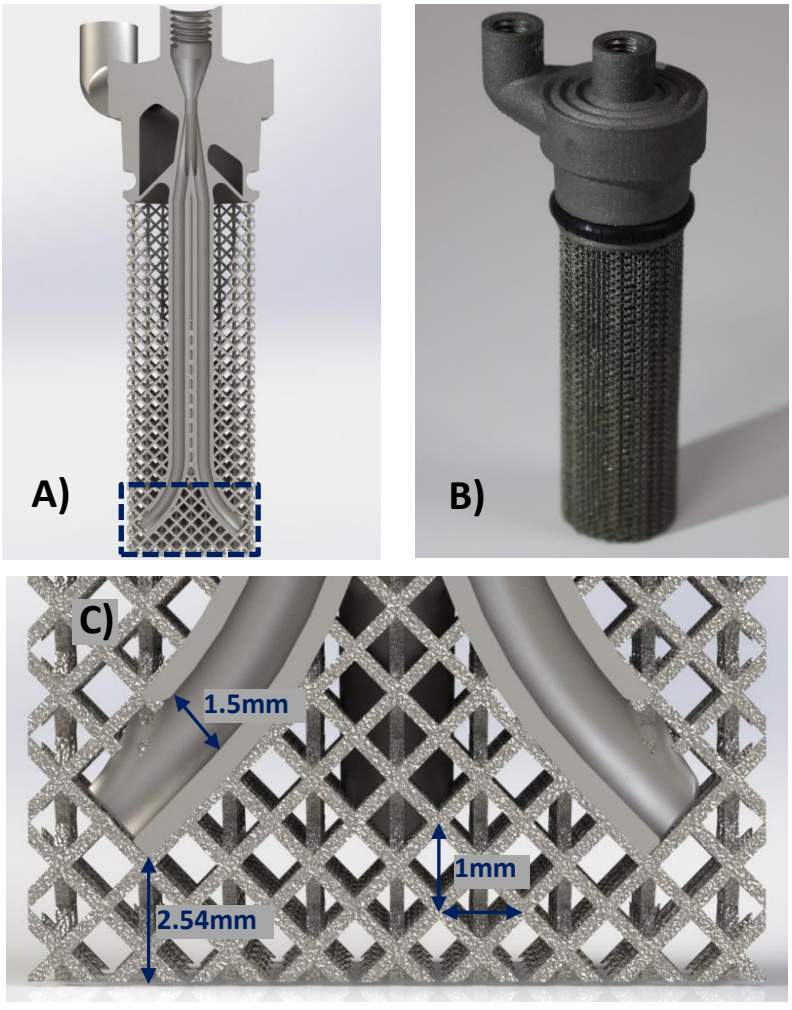

Figure 1 – (a) Cross-sectional rendering of the printed Ti6AL4V electrode structure (simplified lattice structure), (b) Photograph of actual printed device and (c) zoomed section of gas splitter with dimensions.

Prior to being used for HOR, the printed working electrode was coated with Pt by electrodeposition, according to literature methods [30], using a two-step process. Figure S1 shows the current (a) and charge (b) profiles as a function of time during the electrodeposition. Cyclic voltammetry of the Pt coated electrode in an acidic electrolyte (Figure S1c) shows hydrogen adsorption and desorption characteristic peaks similar to those using a Pt sheet (Figure S1d).

For the HOR study, a carbon cloth, also with deposited Pt, and Ag/AgCl (NaCl 3 mol/L) were used as counter and reference electrodes respectively. Hydrogen gas was introduced into the electrolyte through the electrode internal tubes until saturation (determined by the open circuit potential (OCP) plateauing) prior to LSV measurements (Figure 2a). H_2 flow was maintained at 10 ml/min during the LSV experiments, which were made over a potential range from 1 mV more negative than the OCP to 600 mV positive of it, at 50 mV/s. Control experiments were done by purging H_2 directly in the electrolyte next to the printed structure, rather than through the tubes (see inset of Figure 2b).

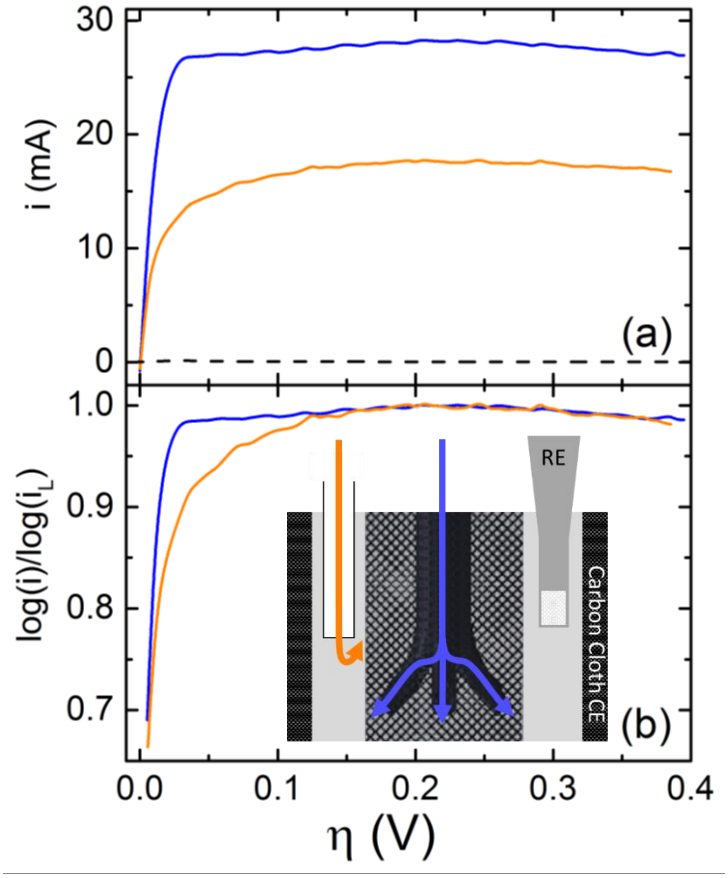

Figure 2: LSV response during HOR, with H_2 either being purged through the internal tubes (blue) or directly into the electrolyte (orange). Operation is shown schematically in inset of (b), with the pathways for H_2 ingress shown using arrows of corresponding colours.

The results presented in Figure 2a show that H_2 oxidation reaches a higher limiting current (i_L) when the gaseous reactant is purged through the 3D printed electrode internal tubes, directly to the active reaction sites. This verifies the assertion that gas reactant transport is a significant impediment to this reaction, as the internal delivery tubes allow the reactant gas to reach the surface of the electrode more efficiently. The limiting current is related to the diffusion layer accordingly to Equation 1 [31].

$$i_L = {}^{nFDC^0}/_{\delta} \qquad (1)$$

Where i_L is the limiting current, n is the number transferred electrons, F is the Faraday constant, D is the diffusion coefficient of the redox specie (cm^2 s), C^0 is the concentration of the redox specie (mol L^{-1}) and δ is the thickness of the diffusion layer. The diffusion layer thickness is the region at which the concentration of the reactant is depleted due its reduction/oxidation. The less efficient the transport of reactants is to the surface of the electrode, the thicker this layer will be. As such, the limiting current is inversely proportional to the diffusion layer thickness. This relationship is independent of the catalytic properties of the electrode and the applied potential, but rather is dependent only on how efficiently reactants are transported. As such, the higher limiting current for the experiments with gas purging through the internal tubes represents a 40% improvement in terms of diffusion of gas reactants to the electrode.

The normalized logarithm of the current with respect to the logarithm of the limiting current, for each electrode, allows us to evaluate the dependence on diffusion on the reaction [28]. The graphs presented in Figure 2b show that for the system with gas delivered directly at the reaction site through the internal tubes of the 3D printed electrode, the limiting current is reached at a lower overpotential (η). It means that the reaction is less dependent on transport limitation and more on the charge transfer rate than when the purging is done directly in the electrolyte.

Conclusions

This work has demonstrated for the first time, to our knowledge, a high surface area, printed electrode with an integrated reactant delivery system. This results in substantial enhancements to the HOR efficiency as compared to gas being delivered external to the electrode structure, where slow diffusion of the gas is limiting. This represents an alternative

to other approaches such GDL, with a greater focus on practicality. This concept may be applied to a range of gas based reactions and helps to demonstrate the array of possibilities for additive manufacturing in electrochemistry applications, which are only just starting to be explored.

Experimental details

Electrode fabrication by selective laser melting:

The electrode (shown in Figure 1) was designed to be produced via the additive manufacturing technique known as SLM. This manufacturing process provides fine spatial resolution producing minimum features of approximately 100µm), thereby lending itself to the production of fine electrode structures exhibiting high surface areas. The equipment used to produce these electrodes (Realizer SLM 50) has a maximum cylindrical build volume, of Ø = 70 mm and height = 74 mm.

The design aim was to maximise reaction surface area within a predefined volume, while providing a staggered path for gas distribution across this high surface area; this volumetric restriction is imposed so the electrode will be compatible with a previously designed reaction vessel. To maximise gas contact area within the electrode, a fine lattice structure was produced with 200 µm diameter cylindrical supports with the unit repeating every 1000 µm. This lattice structure was selected for the electrode body as the resolution was ideal and reliable to produce using SLM and the size of the lattice would create a baffling effect for gas distribution, increasing its diffusion across the electrode.

The basis of the design allows for gas flow into the system via an external connection, and gas out, via an internal chamfered chamber leading to an external connection (seen in Figure 1A). The gas-splitter design has a four-way flow divider to segment flow amongst the

channels (ID 1.5 mm), The internal diameter of the tube has been set to be 50% larger than the lattice spacing in an attempt to further disperse gas flow; this will allow the lattice to both split gas flow on contact with large volume bubbles, but also create a baffling effect with smaller bubbles. Given this anticipated gas distribution effect, four supply outlets have been created, as the resultant gas distribution is not expected to exceed a 90˚ angle.

To achieve the fine resolution required for the electrode lattice, the following laser parameters specific to the Realizer SLM50 are shown below in Table 1:

Table 1: Parameters used in the SLM50 to produce the Ti6Al4V electrode structure

	Pre-hatch	**Hatch**	**Boundaries (Inner and Outer)**
Bed Temperature (ºC)	200		
Oxygen Content (%)	0.2		
Slice Height (µm)	25		
Exposure Time (µs)	60	80	60
Point Distance (µm)	30	40	30
Laser Current (µA)	1700	2500	1700

The produced electrodes were separated from the substrate and sonicated in IPA for one hour to remove any excess, loosely bound, powder which may have been retained from the printing process. Typical abrasive post-processing of SLM parts was avoided as it gives the potential to damage the lattice structure, and/or lodge external contaminant particles into the lattice.

Electrodeposition of Pt on 3D printed electrode:

For the electrodeposition on Pt on the 3D printed electrode the system was first conditioned at +0.3V for 20 s followed by a two-step process: -0.5 V for 50 s and -0.2 V for 150 s. All reported potentials are against a Ag/AgCl NaCl 3 mol L^{-1} reference electrode. As electrolyte, 1 mM $H_2PtCl_6 \cdot 6H_2O$ in 0.1 M KCl solution was used. The same procedure was employed for deposition of Pt on carbon cloth as the counter-electrode.

Hydrogen oxidation reaction experiment:

The HOR experiments were conducted by placing the carbon cloth counter electrode around the 3D printed working electrode, with sufficient spacing to avoid short circuiting. H_2 was then purged either outside the internal tubes or directly into the solution, adjacent to the electrode, until a stable OCP was observed, which took around 20 minutes. The oxidation of H_2 was then studied by linear sweep voltammetry from a potential 1 mV more negative than OCP to +600mV at 50mV/s.

Acknowledgements

This work was supported by the ARC Centre of Excellence for Electromaterials Science (ACES), as well as the Australian National Fabrication Facility (ANFF). AN would like to acknowledge the ARC for funding (DE160100504).

References

1. Baumann, B., et al., *Control of Nanoparticle Release Kinetics from 3D Printed Hydrogel Scaffolds.* Angewandte Chemie International Edition, 2017. **56**(16): p. 4623-4628.
2. Kennedy, Z.C., et al., *3D-printed poly(vinylidene fluoride)/carbon nanotube composites as a tunable, low-cost chemical vapour sensing platform.* Nanoscale, 2017. **9**(17): p. 5458-5466.
3. Sayyar, S., D.L. Officer, and G.G. Wallace, *Fabrication of 3D structures from graphene-based biocomposites.* Journal of Materials Chemistry B, 2017. **5**(19): p. 3462-3482.

4. Hong, S., et al., *Fabrication of 3D Printed Metal Structures by Use of High-Viscosity Cu Paste and a Screw Extruder.* Journal of Electronic Materials, 2015. **44**(3): p. 836-841.
5. Salea, A., et al., *Metal oxide semiconductor 3D printing: preparation of copper(ii) oxide by fused deposition modelling for multi-functional semiconducting applications.* Journal of Materials Chemistry C, 2017. **5**(19): p. 4614-4620.
6. Lee, S., et al., *Three-dimensional Printing of Silver Microarchitectures Using Newtonian Nanoparticle Inks.* ACS Applied Materials & Interfaces, 2017.
7. Ambrosi, A. and M. Pumera, *Self-Contained Polymer/Metal 3D Printed Electrochemical Platform for Tailored Water Splitting.* Advanced Functional Materials: p. 1700655-n/a.
8. Melhem, M.R., et al., *3D Printed Stem-Cell-Laden, Microchanneled Hydrogel Patch for the Enhanced Release of Cell-Secreting Factors and Treatment of Myocardial Infarctions.* ACS Biomaterials Science & Engineering, 2016.
9. Gao, L., et al., *Myocardial Tissue Engineering With Cells Derived From Human-Induced Pluripotent Stem Cells and a Native-Like, High-Resolution, 3-Dimensionally Printed ScaffoldNovelty and Significance.* Circulation Research, 2017. **120**(8): p. 1318-1325.
10. Gu, Q., et al., *3D Bioprinting Human Induced Pluripotent Stem Cell Constructs for In Situ Cell Proliferation and Successive Multilineage Differentiation.* Advanced Healthcare Materials: p. 1700175-n/a.
11. Wallace, G.G., et al., *3D Bioprinting: Printing Parts for Bodies*. 2014, Wollongong: ARC Centre of Excellence for Electromaterials Science. 153.
12. Gupta, V., et al., *3D printed titanium micro-bore columns containing polymer monoliths for reversed-phase liquid chromatography.* Analytica Chimica Acta, 2016. **910**: p. 84-94.
13. Lee, J.-Y., J. An, and C.K. Chua, *Fundamentals and applications of 3D printing for novel materials.* Applied Materials Today, 2017. **7**: p. 120-133.
14. Loo, A.H., C.K. Chua, and M. Pumera, *DNA biosensing with 3D printing technology.* Analyst, 2017. **142**(2): p. 279-283.
15. Cheng, T.S., et al., *3D-printed metal electrodes for electrochemical detection of phenols.* Applied Materials Today, 2017. **9**: p. 212-219.
16. Tan, C., et al., *3D Printed Electrodes for Detection of Nitroaromatic Explosives and Nerve Agents.* Analytical Chemistry, 2017. **89**(17): p. 8995-9001.
17. Lee, K.Y., A. Ambrosi, and M. Pumera, *3D-printed Metal Electrodes for Heavy Metals Detection by Anodic Stripping Voltammetry.* Electroanalysis, 2017. **29**(11): p. 2444-2453.
18. Kwok, S.W., et al., *Electrically conductive filament for 3D-printed circuits and sensors.* Applied Materials Today, 2017. **9**: p. 167-175.
19. Ambrosi, A. and M. Pumera, *3D-printing technologies for electrochemical applications.* Chemical Society Reviews, 2016. **45**(10): p. 2740-2755.
20. Zhao, C., et al., *Three dimensional (3D) printed electrodes for interdigitated supercapacitors.* Electrochemistry Communications, 2014. **41**: p. 20-23.
21. Nathan-Walleser, T., et al., *3D Micro-Extrusion of Graphene-based Active Electrodes: Towards High-Rate AC Line Filtering Performance Electrochemical Capacitors.* Advanced Functional Materials, 2014. **24**(29): p. 4706-4716.
22. Lee, C.-Y., et al., *3D-Printed Conical Arrays of TiO2 Electrodes for Enhanced Photoelectrochemical Water Splitting.* Advanced Energy Materials, 2017. **7**(21): p. 1701060-n/a.
23. Kitson, P.J., et al., *Configurable 3D-Printed millifluidic and microfluidic 'lab on a chip' reactionware devices.* Lab on a Chip, 2012. **12**(18): p. 3267-3271.
24. Parra-Cabrera, C., et al., *3D printing in chemical engineering and catalytic technology: structured catalysts, mixers and reactors.* Chemical Society Reviews, 2018. **47**(1): p. 209-230.

25. Zhakeyev, A., et al., *Additive Manufacturing: Unlocking the Evolution of Energy Materials.* Advanced Science, 2017. **4**(10): p. 1700187-n/a.
26. Kongkanand, A. and M.F. Mathias, *The Priority and Challenge of High-Power Performance of Low-Platinum Proton-Exchange Membrane Fuel Cells.* The Journal of Physical Chemistry Letters, 2016. **7**(7): p. 1127-1137.
27. Greeley, J. and N.M. Markovic, *The road from animal electricity to green energy: combining experiment and theory in electrocatalysis.* Energy & Environmental Science, 2012. **5**(11): p. 9246-9256.
28. Durst, J., et al., *New insights into the electrochemical hydrogen oxidation and evolution reaction mechanism.* Energy & Environmental Science, 2014. **7**(7): p. 2255-2260.
29. Simonelli, M., *Microstructure evolution and mechanical properties of selective laser melted Ti-6Al-4V*. 2014, © Marco Simonelli.
30. Geboes, B., et al., *Electrochemical Behavior of Electrodeposited Nanoporous Pt Catalysts for the Oxygen Reduction Reaction.* ACS Catalysis, 2016. **6**(9): p. 5856-5864.
31. Bard, A.J. and L.R. Faulkner, *Electrochemical Methods: Fundamentals and Applications*. 2001.

Supplemental Information

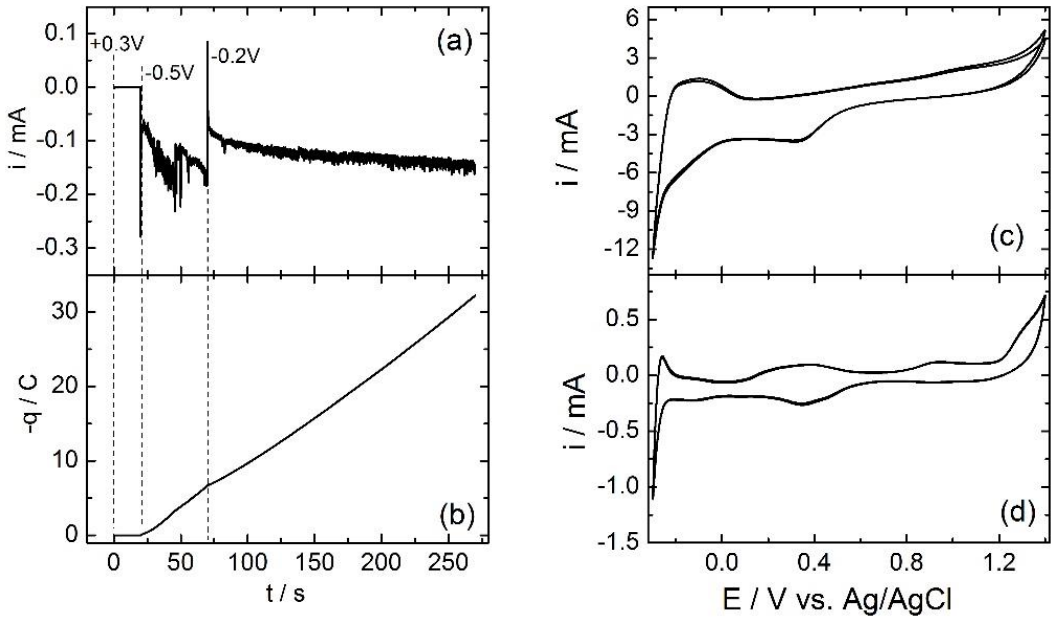

Figure S1: Platinum coating of printed Ti6Al4V structure (a & b) chronoamperometric curve and corresponding total charge curve respectively. (c & d) cyclic voltammetry of Pt coated Ti6Al4V and Platinum mesh to verify the success of the deposition process respectively.